

pubs.acs.org/acschemicalbiology Articles

Refactoring and Heterologous Expression of Class III Lanthipeptide Biosynthetic Gene Clusters Lead to the Discovery of *N,N*-Dimethylated Lantibiotics from Firmicutes

Dan Xue, [#] Zhuo Shang, [#] Ethan A. Older, Zheng Zhong, Conor Pulliam, Kyle Peter, Mitzi Nagarkatti, Prakash Nagarkatti, Yong-Xin Li, and Jie Li*



Cite This: ACS Chem. Biol. 2023, 18, 508-517



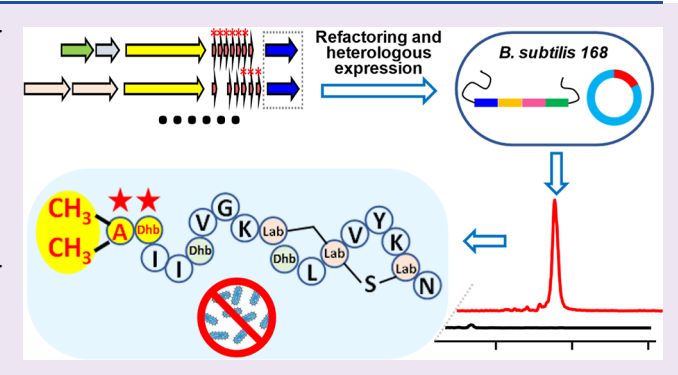
ACCESS

III Metrics & More

Article Recommendations

s Supporting Information

ABSTRACT: Class III lanthipeptides are an emerging subclass of lanthipeptides, representing an underexplored trove of new natural products with potentially broad chemical diversity and important biological activity. Bioinformatic analysis of class III lanthipeptide biosynthetic gene cluster (BGC) distribution has revealed their high abundance in the phylum Firmicutes. Many of these clusters also feature methyltransferase (MT) genes, which likely encode uncommon class III lanthipeptides. However, two hurdles, silent BGCs and low-yielding pathways, have hindered the discovery of class III lanthipeptides from Firmicutes. Here, we report the design and construction of a biosynthetic pathway refactoring and heterologous overexpression strategy which seeks to overcome these hurdles, simultaneously activating and increasing the



production of these Firmicutes class III lanthipeptides. Applying our strategy to MT-containing BGCs, we report the discovery of new class III lanthipeptides from Firmicutes bearing rare N,N-dimethylations. We reveal the importance of the first two amino acids in the N-terminus of the core peptide in controlling the MT dimethylation activity. Leveraging this feature, we engineer class III lanthipeptides to enable N,N-dimethylation, resulting in significantly increased antibacterial activity. Furthermore, the refactoring and heterologous overexpression strategy showcased in this study is potentially applicable to other ribosomally synthesized and post-translationally modified peptide BGCs from Firmicutes, unlocking the genetic potential of Firmicutes for producing peptide natural products.

■ INTRODUCTION

Lanthipeptides are the largest subfamily of ribosomally synthesized and post-translationally modified peptides (RiPPs). These peptide natural products bear characteristic intramolecular lanthionine and/or labionin rings and are often referred to as lantibiotics due to their prevalent antimicrobial properties.^{1,2} They are subdivided into five classes depending on their biosynthetic machinery. 1,3-7 Class III lanthipeptides are an emerging class, beginning with the report of their first member, labyrinthopeptins, in 2010.^{8,9} Consistent with the literature, 10,11 our present bioinformatic analysis of 223,243 bacterial and archaeal genomes revealed that class III lanthipeptide biosynthetic gene clusters (BGCs) are widely distributed in bacterial phyla, with Actinobacteria being the most abundant and Firmicutes being the second most abundant harboring these BGCs. Compared to Actinobacteria, a known major source for class III lanthipeptide discovery, 12-18 no class III lanthipeptide structures had been reported from Firmicutes when we initiated the present study, and now only andalusicin, ¹⁹ amylopeptin, ²⁰ bacinapepand paenithopeptin¹⁰ have been reported, still leaving

class III lanthipeptides in Firmicutes significantly underexplored. In our preliminary screening efforts, lanthipeptide products were not directly detected from almost all the chosen Firmicutes strains harboring class III lanthipeptide BGCs despite various culturing conditions attempted. Thus, two major potential hurdles exist in the exploration of class III lanthipeptides from Firmicutes: (i) No production due to silence of BGCs as generally encountered in natural product discovery^{21–26} and (ii) low-yielding pathways.

To exploit the biosynthetic potential, chemical diversity, and biological activities of these class III lanthipeptides, we designed and established a refactoring and heterologous overexpression strategy using strong inducible promoters,

Received: November 10, 2022 Accepted: February 28, 2023 Published: March 9, 2023





efficient ribosome-biding sites (RBSs), and high-copy-number plasmids. This strategy simultaneously activates and increases compound production, enabling discovery, isolation, characterization, and further biological evaluation. We applied this strategy to a unique group of Firmicute class III lanthipeptide BGCs featuring uncommon MTs, leading to the discovery and characterization of new representative class III lanthipeptides. These new lanthipeptides all feature rare *N*,*N*-dimethylations, installed by the MTs. We further revealed the importance of the first two amino acids in the *N*-terminus of the core peptide for the observed *N*,*N*-dimethylation activity. Leveraging this observation, we engineered class III lanthipeptides to enable *N*,*N*-dimethylation, resulting in a significantly increased antibacterial activity.

RESULTS AND DISCUSSION

Genome Mining of Class III Lanthipeptides and Design of a Refactoring and Heterologous Overexpression Strategy. We analyzed 223,243 bacterial and archaeal genomes using antiSMASH 6.0 and identified 3897 and 570 class III lanthipeptide BGCs from Actinobacteria and Firmicutes, respectively (Supporting Information, Data File S1). Among these, ~35% of class III lanthipeptide BGCs from Firmicutes contains a gene encoding a SAM-dependent MT (Figure 1A), while only two of such BGCs had been connected to their chemical products. ^{10,19} In the phylogenetic analysis of all reported RiPP SAM-dependent MTs, we discovered that those in Firmicute class III lanthipeptide BGCs form a distinct clade, separate from reported SAM-dependent MTs involved in the biosynthesis of Firmicute-derived other RiPPs (e.g., PtnL²⁷), non-Firmicute-derived lanthipeptides (e.g., LxmM⁵), and non-Firmicute-derived other RiPPs (e.g., SinM²⁸ and MonM²⁹) (Figure S1). We hypothesized that these MTcontaining class III lanthipeptide BGCs may encode new types of methylated products specific to class III lanthipeptides from Firmicutes. Further bioinformatic analysis revealed that nearly 25% of them contained multiple precursor peptides with identical core peptide sequences, some with up to six identical copies (Figure 1A), suggesting a potential evolutionary importance in having additional copies to encode the desired methylated products.

However, no lanthipeptide products were detected from nearly all of the 20 Firmicute strains containing class III lanthipeptide BGCs that we directly cultivated under various culturing conditions (Supporting Information, Table S1). Thus, we set out to devise a refactoring and heterologous overexpression strategy. Previously reported Firmicute class III lanthipeptide heterologous expression systems involve a single plasmid (either a replication plasmid pHT0119 or an integrative plasmid pDR111¹⁰) for the expression of both precursors and PTM enzymes. Using a replication plasmid could facilitate high expression levels, while an integrative plasmid provides high stability for expression by integrating genes into the genome of the host. Thus, we developed a refactoring and heterologous overexpression strategy by leveraging the advantages of both types of plasmids (Figure 1B): (1) precursor peptides are expressed in a high-copynumber replication plasmid, pBS0E, which contains the xyloseinducible promoter P_{xylA} . This is intended to mirror the higher transcription rate of the repeated precursor peptides in the BGCs as well as to further increase the precursor peptide expression level and (2) the genes encoding lanthipeptide PTM enzymes (i.e., lanthipeptide synthetases LanKC, MT

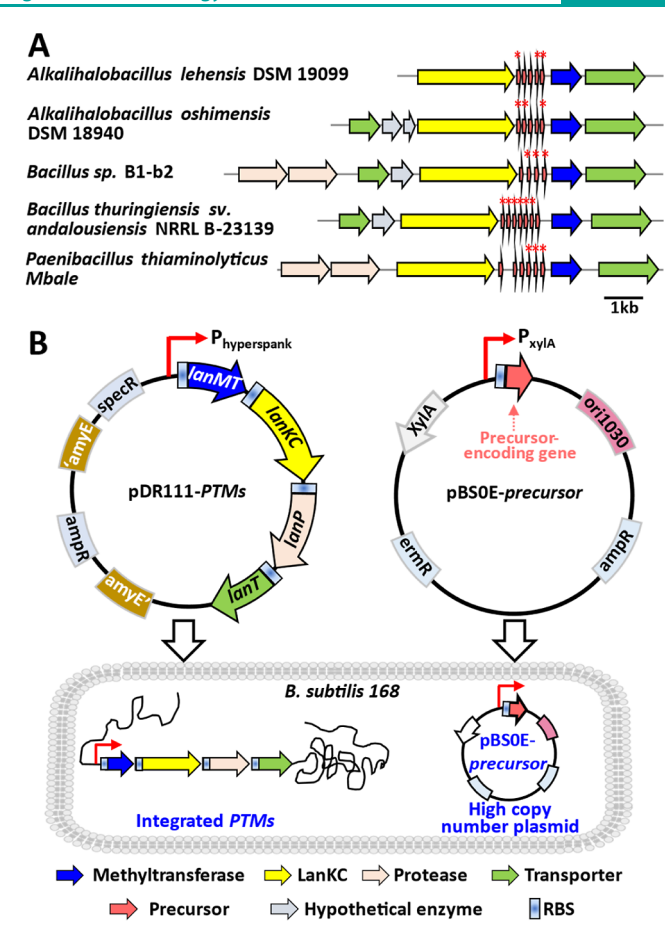


Figure 1. (A) Representative MT-containing class III lanthipeptide BGCs from Firmicutes found through bioinformatic analysis. Identical repeated precursor peptide sequences are marked with a red asterisk ("*"). (B) General scheme of our biosynthetic pathway refactoring and heterologous overexpression strategy, including two central components: pDR111 containing lanthipeptide post-translational modification (PTM) enzyme-encoding genes (lanMT for MT, lanKC for lanthipeptide synthetase, lanP for protease, and lanT for transporter) and pBS0E containing the interchangeable lanthipeptide precursor-encoding gene. pDR111-PTMs integrates the PTM enzyme-encoding genes into the Bacillus subtillis (B. subtilis) 168 chromosome, and the pBS0E-precursor is subsequently transformed into the integrated host.

LanMT, protease LanP, and transporters LanT) are integrated into the genome of a B. subtilis host, to provide higher expression stability, under the control of the strong IPTG-inducible promoter, $P_{\rm hyperspank}$, using an integrative plasmid, pDR111. Precursors and PTM enzyme-encoding genes are each preceded by the B. subtilis mntA RBS (AAGAGGAGG), which is considered as a strong Shine-Dalgarno sequence ($\Delta G > 50.4 \ \rm kJ \ mol^{-1}$). A spacing of six nucleotides (AGAAAT) to the starting codon is employed to ensure translation efficiency. Our system is also modular, allowing the facile expression of different precursor peptides from the same BGC while using the same engineered heterologous host with integrated PTM-encoding genes. This feature will be useful for studying class III lanthipeptide BGCs with multiple encoded precursor peptides.

Heterologous Overexpression Leads to the Discovery of New N,N-Dimethylated Class III Lanthipeptides from Firmicutes. We identified a representative MT-containing BGC (ptt) from Paenibacillus thiaminolyticus NRRL B-4156

(Figure 2A), which contains the MT-encoding gene (pttMT) and duplication of precursor-encoding genes (pttA5 and its

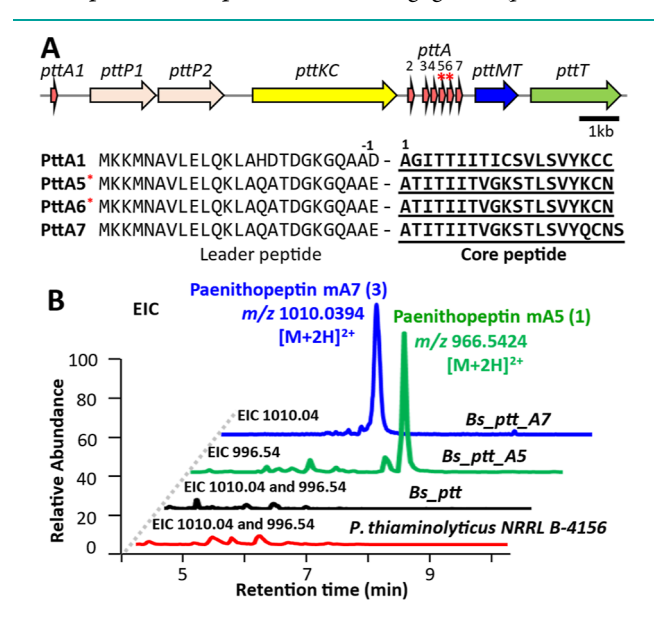


Figure 2. (A) Overview of the *ptt* BGC displaying each biosynthetic gene, including the MT-encoding *pttMT*. The identical repeated precursor-encoding genes *pttA5* and *pttA6* are marked with a red asterisk ("*"). (B) Extracted ion chromatograms from the liquid chromatography—mass spectrometry (LC—MS) analysis of heterologous overexpression hosts *Bs_ptt_A5* and *Bs_ptt_A7* demonstrate the significantly increased production of 1 (green) and 3 (blue), respectively, compared to the native strain (red) and empty host (black).

additional identical copy, pttA6). We applied the refactoring and heterologous overexpression strategy described above to activate and improve lanthipeptide production derived from PttA5 (Supporting Information, Figure S2 and Tables S1 and S2). LC-MS analysis of the extract of the PttA5 heterologous expression strain (Bs_ptt_A5, Supporting Information, Figure S3) revealed the high-yield production of a peptide-like, multiply charged ion with a molecular weight of 1931.1 Da which was not present in the negative control strain containing no ptt precursor (Figures 2B and S3). The mass-to-charge ratio (m/z) of this differential peak was +28 Da from the bioinformatically predicted molecular weight of mature PttA5, suggesting that the product may be dimethylated. We named this compound paenithopeptin mA5 (1, Figure 3A). We next isolated 1 and characterized its structure using nuclear magnetic resonance (NMR), high-resolution tandem mass spectrometry (HRMS/MS), and chemical derivatization, along with bioinformatic prediction of the core peptide sequence. HRMS showed the presence of a doubly charged protonated ion $[M + 2H]^{2+}$ with m/z 966.5424 (calcd m/z 966.5424) indicative of the molecular formula C₉₁H₁₄₆N₂₂O₂₂S (Figure S3). 1D NMR (DMSO- d_6) analysis of 1 exhibited resonances of four olefinic protons ($\delta_{\rm H}$ 6.30–6.40 ppm, q, J = 6.9 Hz; $\delta_{\rm C}$ 127.6–129.2 ppm) and two pairs of aromatic protons ($\delta_{\rm H}$ 6.64 and 6.95 ppm, d, J = 8.1 Hz; $\delta_{\rm C}$ 115.5 and 130.5 ppm), suggesting the presence of four dehydrobutyrine (Dhb) residues and one tyrosine residue (Figures S4 and S5). These findings are consistent with the core peptide sequence of 1 which contains four threonines and one tyrosine, of which threonine undergoes dehydration by PttKC to yield Dhb.

Finally, the resonances of two chemically equivalent N-methyl groups ($\delta_{\rm H}$ 2.23 ppm, s; $\delta_{\rm C}$ 41.7 ppm) were observed and also showed heteronuclear multiple bond correlation (HMBC) with the α -carbon (δ_C 63.2 ppm) of the first alanine residue (Ala1), confirming the hypothesized N,N-dimethylation of Ala1 (Figures 3B and S6-S11 and Table S3). Elaborating on the structure of 1, collision-induced dissociation tandem mass spectrometry (CID-MS/MS) was applied, and a series of b ions (N-terminal sequence retained) and y ions (C-terminal sequence retained) were generated (Figures 3C and S3). Manual annotation of the fragment ions confirmed the presence of an N,N-dimethylated Ala1 and three Dhb residues (Dhb2, Dhb4, and Dhb7). Moreover, the MS/MS fragmentation of 1 terminated at Ser11 even under high collision energy (50 eV), suggesting that Ser11 may be involved in lanthionine (Lan) or labionin (Lab) ring formation. Given the very similar C-terminal sequence of the core peptides in 1 (STLSVYKCN) and paenithopeptin A (2, SVLSVYKCC) that we previously discovered, 10 we hypothesized that a bicyclic labionin ring formed between Ser11, Ser14, and Cys18 in the structure of 1, as it does in 2.10 The presence of a labionin bicyclic ring was subsequently confirmed by the following evidence. First, when compared to the partial core peptide sequence STLSVYKCN (m/z 1014.49), the y9 ion revealed a diagnostic loss of 54 Da (m/z 960.46) (Figure 3C) corresponding to triple dehydrations, suggesting the formation of one Dhb and two Dha residues in the y9 ion. Second, when 1 was treated with β mercaptoethanol (β -ME) (Figure S12), β -ME adducts were not detected that indicates the absence of free Dha in the structure. This lack of free Dha suggests that Dha residues are involved in the formation of a labionin ring as previously described. 14,17 Most importantly, LC-HRMS analysis of the Ntrifluoroacetyl/ethylester derivatives of the acid hydrolysate of 1 returned two peaks bearing ions at m/z 668.1320 [M + H]⁺ (calcd m/z 668.1319, -0.15 ppm) and at m/z 668.1317 [M + H^{+} (calcd m/z 668.1319, +0.30 ppm), respectively, corresponding to the molecular formula C₂₁H₂₆F₉N₃O₉S⁺ (Figure S13), which represents the N-trifluoroacetyl/ethylester of labionin (Figure S14). 14,31 The presence of two peaks corresponding to labionin is consistent with epimerization of the residue during hydrolysis as previously reported. 14,31 Further MS/MS analysis of the ion at m/z 668.1320 yielded the diagnostic fragments that match those previously reported (Figure S14), 14,31 confirming the presence of a labionin bicyclic ring in 1. The absolute configurations of each residue in 1 were determined to be the L-configuration by Marfey's analysis (Table S4). All of the evidence stated above indicated 1 as a new N,N-dimethylated class III lanthipeptide with a bicyclic labionin ring.

With the successful activation and production of 1, we next expanded our strategy to another precursor peptide, PttA7, in the same ptt BGC (Figure 2A). Heterologous expression of the PttA7 precursor led to the identification of another N_iN_i -dimethylated class III lanthipeptide, paenithopeptin mA7 (3). Analysis of the PttA7 heterologous expression strain (Bs_ptt_A7) extract by HRMS revealed a doubly charged protonated ion [M + 2H⁺]²⁺ with m/z 1010.0394 (calcd m/z 1010.0402, +0.79 ppm) indicative of the molecular formula $C_{93}H_{147}N_{23}O_{25}S$ (Figure S15). The core peptide sequences of PttA7 and PttA5 are very similar, with the only difference being the replacement of Lys17 with Gln17 and the addition of Ser20 in 3. CID-MS/MS analysis of 3 revealed identical b ions to those of 1 and +87 Da in the y ions, which was attributed to

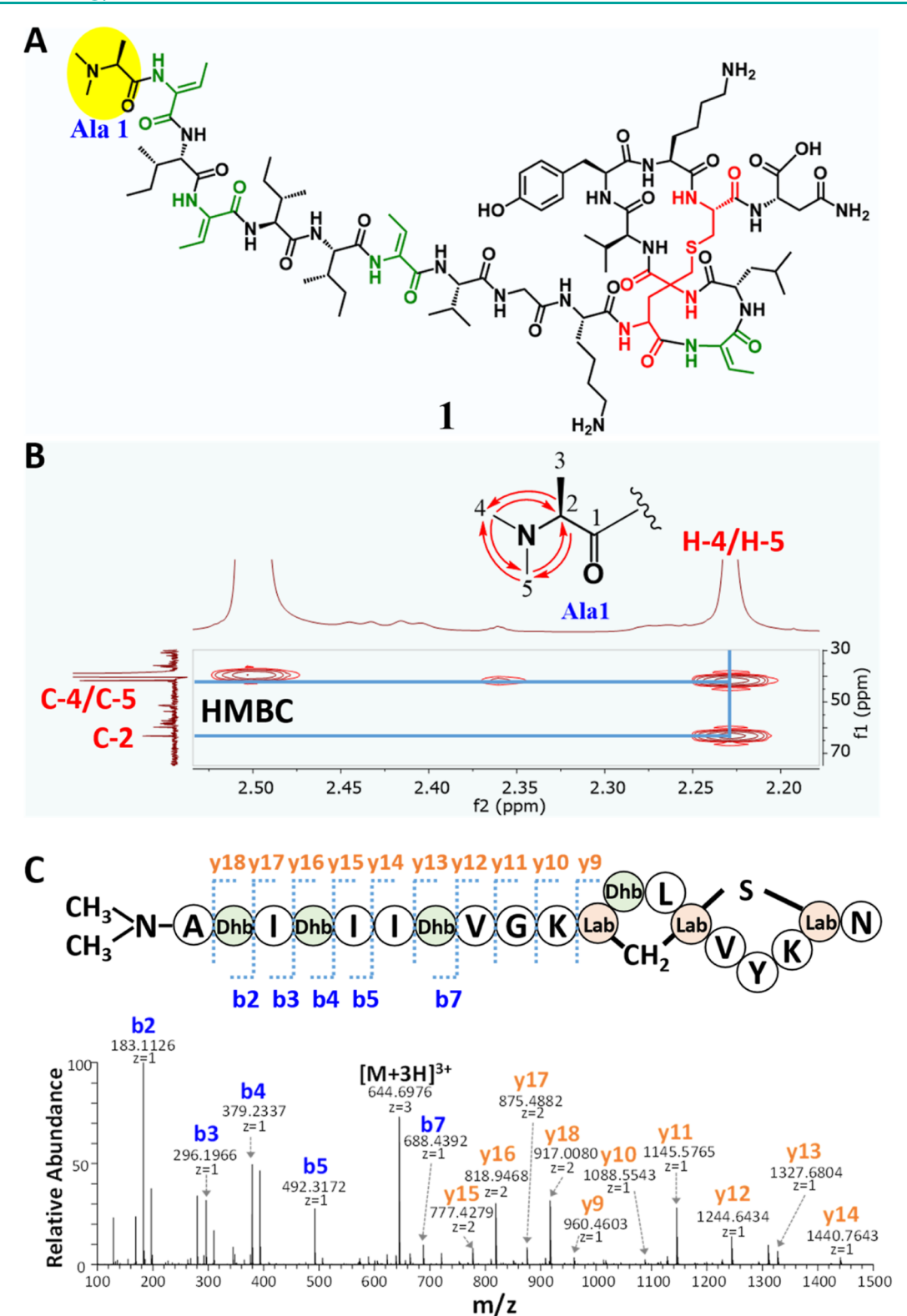


Figure 3. (A) Chemical structure of **1.** Dhb residues are in green, and Ser and Cys involved in the labionin ring are in red. (B) Selected key HMBC correlations indicating *N*,*N*-dimethylation of Ala1. (C) Amino acid sequence of **1**, showing the CID-MS/MS fragmentation patterns and representative MS/MS spectra used to confirm the amino sequences and to determine the position of the labionin ring.

the change in molecular mass from Gln17 and Ser20 in 3 (Figure 4). These results indicated 3 as bearing a labionin ring formed between Ser11, Ser14, and Cys18.

We compared the production yields between the newly developed two-plasmid (pDR111 and pBS0E) refactoring

strategy and previous one-plasmid (pDR111) expression system. The new strategy not only significantly improved the production of 2 but also activated the production of 1 and 3 compared to that using the previous heterologous expression system that integrated the entire BGC in the host genome ¹⁰

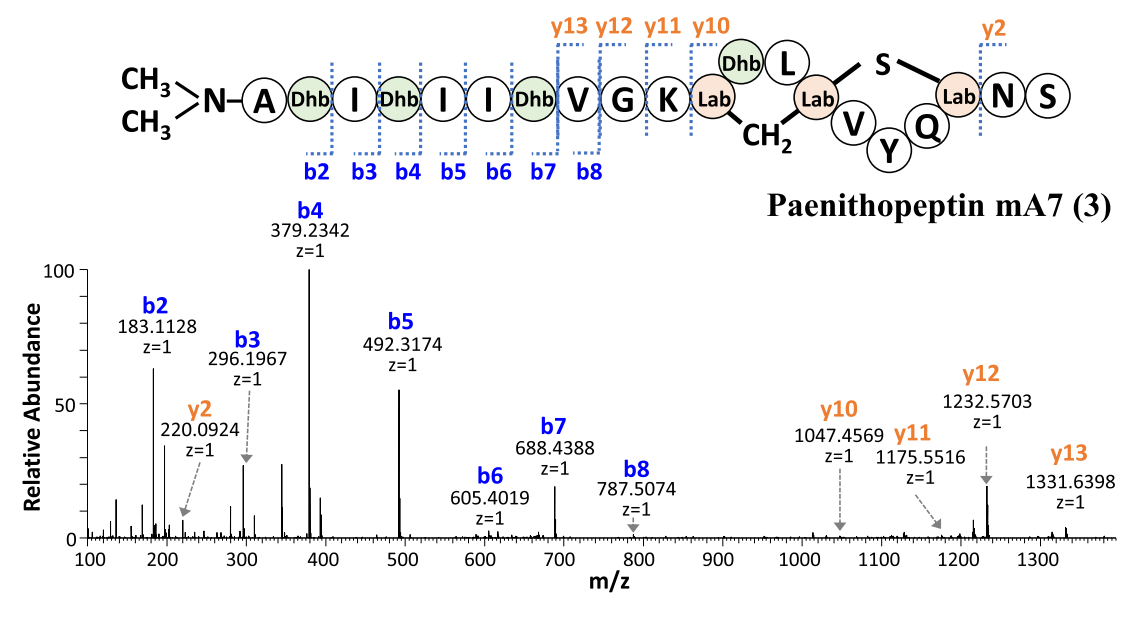


Figure 4. Amino acid sequence of 3, showing the CID-MS/MS fragmentation patterns and representative MS/MS spectra used to confirm the amino sequences and to determine the position of the labionin ring.

(Figure S16). To further apply our strategy, we selected another MT-containing BGC, ben from Bacillus nakamurai NRRL B-41092, which we previously reported to produce only very low yields of the corresponding products by native strain cultivation.¹⁰ Notably, the bcn BGC harbors no protease genes that are required for lanthipeptide maturation but are lacking in the majority of class III lanthipeptide BGCs. Instead, the distal proteases identified elsewhere in the genome using our previously reported correlational networking approach 10 were used in the heterologous expression system. Overexpression of the precursors, BcnA1 and BcnA2, and induction of their respective biosynthetic genes including the distal protease genes led to significantly increased production of both products bacinapeptins A (4) and B (5) compared to the native strain production (Figure S17), and structural analysis by CID-MS/MS matched our previously reported data. 10 All the aforementioned successful examples demonstrate that our refactoring and heterologous overexpression strategy is generally applicable to a broad range of Firmicute class III lanthipeptide BGCs using pathway-specific proteases or distal proteases identified via correlational networking. 10

Importance of the First Two Amino Acids in the N-Terminus of the Core Peptide for N,N-Dimethylation by PttMT. Although heterologous overexpression of pttA5 and pttA7 led to the production of 1 and 3, respectively, overexpression of pttA1 using the same strategy surprisingly did not result in the biosynthesis of N,N-dimethylated 2 (Figure S18). Given that the methylation reaction occurs after the removal of the leader peptide by the protease, we predicted that the amino acids in the N-terminus of the core peptide may be important determinants in influencing PttMT activity. Thus, we aligned the core peptide sequences of previously reported RiPPs bearing the N,N-dimethylation moiety. According to the alignment, the second amino acid in the core peptide is strictly conserved to Thr or Ser (Figure 5A). It is well-known that Thr and Ser are the only β -hydroxy-bearing amino acids that can be enzymatically dehydrated to generate Dhb and dehydroalanine (Dha), respectively, in the biosynthesis of lanthipeptides and linaridins. Therefore, we

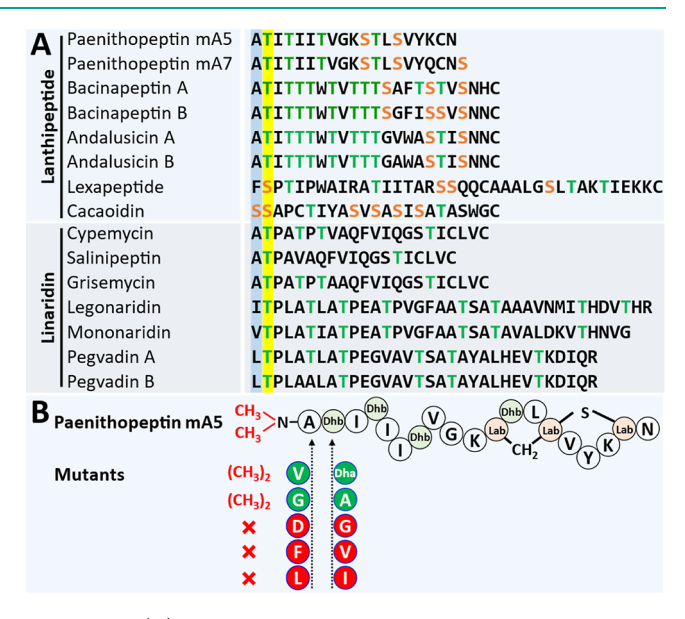


Figure 5. (A) Aligned lanthipeptide core peptide sequences highlighting the first two highly conserved N-terminus amino acids. We find that these two residues are conserved not only in N_iN_j -dimethylated lanthipeptides but also in dimethylated linaridins. (B) Mutagenesis of the first two residues to other amino acids demonstrates the importance of these two positions in controlling the N_iN_j -dimethylation activity of PttMT.

hypothesized that the dehydrated amino acids Dhb and Dha in the second position of the core peptide are essential for recognition and methylation. To probe the importance of this position in *N*,*N*-dimethylation, we created a variety of PttAS mutants with changes to the second amino acid (representative mutants are shown in Figure 5B). The mutated *pttAS* gene was subsequently coexpressed with *pttMT* and other lanthipeptide biosynthetic genes using the aforementioned heterologous expression system, followed by LC–MS analysis. The results clearly showed that the T2S and T2A mutants retained *N*,*N*-dimethylation (Figures S19–S21), giving paenithopeptin mA5 T2S (6) and paenithopeptin mA5 T2A (7), respec-

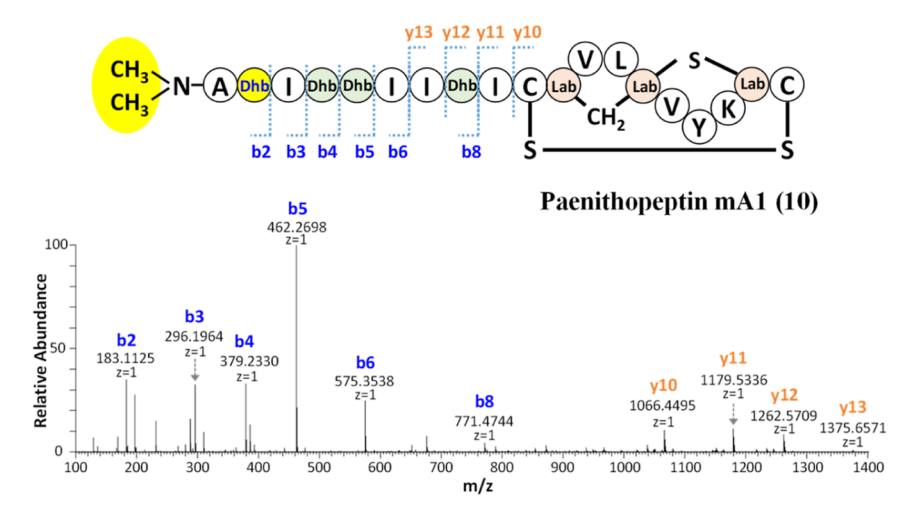


Figure 6. Amino acid sequence of **10** obtained after mutation of the second amino acid, Gly2 to Thr2, resulting in PttMT methylation activity. The *b* and *y* fragmentation sites are indicated on the structure, and representative CID-MS/MS spectra are shown which were used to confirm the structure of **10**.

tively. However, other mutants such as T2G, T2V, and T2I did not (Figure S19), suggesting that PttMT prefers neutral amino acids bearing a small aliphatic side chain of up to two carbons such as Ala, Dhb, and Dha.

While the first amino acid is not as conserved as the second, Ala1 is found in more than half of known *N*,*N*-dimethylated RiPPs (Figure 5A). Thus, we next generated several mutants of the first amino acid in PttA5. Our analysis revealed that the A1G and A1V mutants did not affect *N*,*N*-dimethylation of the core peptide, leading to paenithopeptin mA5_A1G (8) and paenithopeptin mA5_A1V (9), respectively (Figures S22—S24). In contrast, changing Ala1 to the bulky amino acids Leu or Phe, as well as the polar amino acid Asp, abolished *N*,*N*-dimethylation (Figures 5B and S22). Our mutagenesis results demonstrated that PttMT has modest substrate specificity, accepting neutral amino acids with small aliphatic side chains in the first and second positions.

To leverage this feature, we engineered the precursor peptide sequence of PttA1, which is not naturally methylated, by mutating the second amino acid of the core peptide from Gly to Thr. Coexpression of the mutated pttA1 along with pttMT and other essential biosynthetic genes in our heterologous host indeed yielded a new N,N-dimethylated peptide, namely, paenithopeptin mA1 (10), which showed a doubly charged protonated ion $[M + 2H]^{2+}$ at m/z 961.5052 (calcd m/z 961.5061, +0.92 ppm), suggestive of the molecular formula C₉₁H₁₄₄N₂₀O₂₁S₃ (Figure S25). CID-MS/MS analysis of 10 exhibited a b2 ion (m/z 183.11) that is 54 Da larger than that for 2, 10 the mass increase of which can be attributed to the replacement of Gly with Dhb and the addition of two methyl groups (Figure 6). Our study provides an opportunity for the use of PttMT as a biocatalyst to produce non-natural lanthipeptides with increased antibiotic activity as described below.

N,N-Dimethylation Enhances the Antibacterial Activity of Class III Lantibiotics. *N,N*-dimethylation is a rare posttranslational modification in RiPP biosynthesis, which has been linked to increased biological activities, while demethylation has shown reduced biological activities. For example, the *N,N*-demethylated forms of cypemycin, andalusicin, and plantazolicin all had lost or significantly reduced antibacterial activity. ^{19,27,32} To validate the significance of *N,N*-dimethyla-

tion on the activity of paenithopeptins, we assayed the antibacterial activity of 1 and 10 as well as their demethylated forms, paenithopeptin A5 (11) and 2, that were discovered in our previous research, ¹⁰ respectively, using an agar diffusion assay. The results clearly showed that 1 and 10 had significantly more potent inhibitory activity against Grampositive bacteria in comparison to their demethylated counterparts (Table 1), confirming the important role of N,N-

Table 1. Antibacterial Activity of Paenithopeptins^a

	Paenithopeptins				
strains	mA5 (1)	A5 (11)	mA1 (10)	A (2)	Ampicillin
Staphylococcus aureus RN4220	+	-	+	-	+
Enterococcus faecium EF16	+	-	+	_	+
Bacillus subtilis ATCC6633	+++	+	+	_	++
Paenibacillus durus DSM5976	+++	+	+++	+	+
Paenibacillus odorifer DSM15391	+++	+	+++	+	+
Escherichia coli DH5a	_	_	_	_	+++

"Growth inhibition zones were measured to indicate relative inhibitory activity strength. "—" indicates no observed inhibitory activity; "+" corresponds to low inhibitory activity (growth inhibition zone diameter is between 1 and 2 cm); and "+++" corresponds to strong inhibitory activity (growth inhibition zone diameter is greater than 4 cm). Ampicillin was used as the positive control. The blank solvent was used as the negative control and showed no inhibition zone.

dimethylation in the antibiotic effect of paenithopeptins. *N*-methylation could significantly improve the stability and pharmacological properties of RiPPs by preventing proteolytic degradation and potentially enhancing membrane penetration and thus may endow the RiPPs with stronger antibacterial activities. Like the majority of lantibiotics that tend to significantly inhibit the growth of bacteria in the same genus as the lantibiotic-producing strain, we observed that paenithopeptins showed antibiotic activity against the genus *Paenibacillus* and the closely related *Bacillus* genus.

CONCLUSIONS

In this study, we identified abundant class III lanthipeptide BGCs derived from Firmicutes containing uncommon MTencoding genes and frequently bearing additional identical precursor peptide copies. Leveraging the modularity of RiPP biosynthesis, we designed and established a biosynthetic pathway refactoring and heterologous overexpression strategy allowing the activation and increased production of new class III lanthipeptides, such as 1 and 3 both bearing rare N,Ndimethylations. We revealed the importance of the first two amino acids in the N-terminus of the class III lanthipeptide core peptide in controlling N,N-dimethylation activity, and we further demonstrated that engineering a precursor peptide at these positions can enable N,N-dimethylation, resulting in significantly increased antibacterial activity. While we designed and applied this strategy to Firmicute class III lanthipeptides, we envision that our methodology can easily be applied to a broad range of other Firmicute RiPP BGCs, unlocking the potential of these promising natural products.

MATERIALS AND METHODS

General Materials, Reagents, and Strains. Chemical reagents, biochemicals, and media components used in this study were purchased from Thermo Fisher Scientific Co. Ltd. (USA) unless otherwise stated. Restriction endonucleases were purchased from New England Biolabs, Inc. (USA). PrimeSTAR HS DNA polymerase (Takara Biotechnology Co., Ltd. Japan) was used for all polymerase chain reaction (PCR) amplifications on an Eppendorf Mastercycler Nexus X2 Thermal Cycler (Eppendorf Co., Ltd. Germany). PCR products were purified using the E.Z.N.A. Gel Extraction Kit (Omega Bio-tek, Inc., USA). The NEBuilder HiFi DNA Assembly master mix (New England Biolabs, Inc., USA) was applied for Gibson assembly. All plasmids were extracted using the E.Z.N.A. Plasmid DNA Mini Kit I (Omega Bio-tek, Inc., USA). Oligonucleotide synthesis and DNA sequencing were performed by Eton Bioscience, Inc. (USA). Genes were synthesized by GenScript, Inc. (USA). All strains used in this study are listed in Table S1.

Identification of BGCs and MT. All publicly available bacterial genomes were downloaded from the NCBI RefSeq database (n = 223,243, accessed in Aug. 2021) and analyzed by antiSMASH 6.0 with default parameters. Lanthipeptide BGCs, subclasses, and precursors were annotated by antiSMASH automatically based on sequence homology to known BGCs and biosynthetic enzymes. MTs in lanthipeptide BGCs were identified and extracted by searching for gene annotations including "MT" in antiSMASH-generated output files. Resulting BGCs were collected in Microsoft Excel, along with related information including lanthipeptide precursor peptide sequences, originating genome name, assembly accession, and taxonomy (Data File S1).

Phylogenetic tree analysis involving 16 MTs was performed using the Neighbor-Joining method.³³ The tree is drawn to scale, with branch lengths in the same units as those of the evolutionary distances used to infer the phylogenetic tree. The percentage of replicate trees in which the associated taxa clustered together in the bootstrap test (1000 replicates) is shown next to the branches. The evolutionary distances were computed using the Poisson correction method and are in the units of the number of amino acid substitutions per site. All ambiguous positions were removed for each sequence pair (pairwise deletion option). Evolutionary analyses were conducted in MEGA11.³⁴

Cloning and Engineering of *B. subtilis* Strains. To construct the pDR111 plasmids containing PTM-encoding genes, the vector, pDR111, was digested with SalI and SphI. Genes in the *ptt* BGC (*pttMT*, *pttKC*, *pttP1*, *pttP2*, and *pttT*) and *bcn* BGC (*bcnMT*, *bcnKC*, *bcn-gP1*, and *bcn-gP2*) were PCR-amplified from the genomic DNA of *P. thiaminolyticus* NRRL B-4156 or *B. nakamurai* NRRL B-41092, respectively. The mntA ribosome-binding site plus a spacer sequence

(AAGAGGAGAAAT) was added upstream of the coding region via PCR. PCR products containing appropriate homologous overhanging regions were assembled with linearized pDR111 via Gibson assembly, generating pDR111-pttPTMs and pDR111-bcnPTMs.

The pBS0E plasmids containing precursor-encoding genes were also constructed via Gibson assembly. The precursor-encoding gene was synthesized (with the start codon GTG changed to ATG to better accommodate to the heterologous host *B. subtilis* 168^{35,36}) and amplified with appropriate overhangs for Gibson assembly, and the pBS0E vector was linearized by digestion with EcoRI and SphI. All cloning steps were performed in *Escherichia coli* DH10B, and all the generated recombinant plasmids were confirmed by sequencing. Primers used for PCR are listed in Table S2.

Mutagenesis of *pttA5* and *pttA1* was performed by PCR-based site-directed mutagenesis.³⁷ The wild-type *pttA5* gene was amplified via PCR with primers containing the desired base changes (Table S2). Mutated PCR products were used for Gibson assembly with linearized pBS0E, as described above, to generate plasmids containing mutations (Table S1).

The plasmids pDR111 containing PTM-encoding genes were integrated into the chromosome of B. subtilis_\Delta ymfFH, lacking the genes ymfF and ymfH which are homologous to the proteases used by the ptt and bcn BGCs, 10 generating the Bs ptt and Bs bcn strains. Briefly, B. subtilis_\Delta ymfFH was cultured overnight in Luria-Bertani (LB) broth and then diluted to $OD_{600} = 0.1$ in a total volume of 400 μL transformation medium (6.5 mM K₂HPO₄·3H₂O, 4.8 mM KH₂HPO₄, 0.37 mM Na-citrate 2H₂O, 2% glucose, 0.2% Kglutamate, 0.01 mg/ml Fe[III]-ammonium-citrate, and 0.05 mg/mL tryptophan) and incubated for 4 h at 37 °C, with shaking at 220 rpm. Then, 200 ng of plasmid DNA was added to the culture and incubated for 1 h before the addition of 100 μ L of expression mix (2.5% yeast extract, 2.5% casamino acid, and 0.25 mg/mL tryptophan). Following another 1 h of incubation, the culture was plated on LB agar supplemented with spectinomycin (100 μ g/mL). After overnight incubation at 37 °C, single colonies were selected, and positive integration was confirmed using colony PCR. Then, pBS0E constructs containing precursor peptide-encoding genes were individually transformed into the Bs_ptt or Bs_bcn host using the same protocol described above.

Lanthipeptide Production and Extraction. The lanthipeptide heterologous expression strains were inoculated in a culture tube containing 2 mL of tryptic soy broth (TSB) and shaken at 220 rpm, 37 °C, overnight, to serve as a seed culture. The seed culture was then diluted 100 times into 30 mL of TSB in 150 mL Ultra Yield flasks (3×) and subsequently shaken at 220 rpm, 37 °C until the OD₆₀₀ reached 0.7. Then, the cultures were induced using 1% xylose and 1 mM IPTG. After induction, the cultures were grown for 3 days at 20 °C with shaking at 220 rpm. The bacterial broth was then extracted with 10 mL of butanol, and the organic phase was evaporated under $\rm N_2$. Extracts were redissolved in MeOH to a concentration of 10 mg/mL for LC–MS analysis.

Isolation of 1 and 10 from Heterologous Expression **Strains.** The heterologous expression host *Bs_ptt_A5* was inoculated in 500 mL of TSB in 10 2.5 L Ultra Yield flasks for a total of 5 L of TSB and induced using the same method described above. The cultures were grown for 3 days at 20 °C with shaking at 220 rpm. The culture broth was extracted with an equal volume of butanol, and the combined organic phases were concentrated in vacuo. The resulting crude extract (7 g) was then partitioned on a reversed-phase C18 open column with a 25% stepwise gradient elution from 50% H2O/ MeOH to 100% MeOH. Pure MeOH with 1% formic acid was applied for an additional final elution. The MeOH/formic acid fraction (332 mg) was further purified by semipreparative highperformance liquid chromatography (HPLC) (Thermo Dionex Ultimate 3000 HPLC system with Chromeleon 7.2.10) on a Phenomenex Luna RP-C18 column (250 \times 10 mm, 5 μ m, 100 Å) using an isocratic elution at 28% H2O/MeCN over 30 min with constant 0.1% formic acid and a flow rate of 3.5 mL/min to yield 1 (36 mg). Lanthipeptide 10 was isolated following the same procedure using Bs ptt A1 G2T strain.

High-Resolution ESI-MS and CID-MS/MS Analysis of Lanthipeptides. A Thermo Scientific Q-Exactive HF-X hybrid Quadrupole-Orbitrap mass spectrometer was used for the highresolution electrospray ionization (ESI)-MS spectra and CID-MS/MS analysis of paenithopeptins using ESI in the positive ion mode. LC was performed on a Thermo Vanquish HPLC interfaced to the aforementioned mass spectrometer. A Thermo Scientific ProSwift RP-4H reversed-phased monolith column with dimensions 1×250 mm was used for the separation. Solvent A was 0.1% formic acid in water and solvent B was 0.1% formic acid in acetonitrile, with the flow rate being 200 μ L/min. The LC gradient used started at 10% B for 1 min and then increased to 100% B over 10 min where it remained for 5 min. MS1 scans were obtained in the orbitrap analyzer which scanned from 500 to 2000 m/z at a resolution of 60,000 (at 200 m/z). For CID-MS/MS, the relevant parent ion was selected with a 2 m/zwindow and fragmented by CID using normalized collision energies of 20, 25, and 30 eV (results were combined into one spectrum). Fragment ions were then sent to the Orbitrap for mass analysis at 30,000 resolution. The MS data was analyzed by Thermo Xcalibur (4.2.47).

NMR Characterization of 1. Lanthipeptide 1 was dissolved in DMSO- d_6 for 1 H, 13 C, 1 H- 1 H COSY, 1 H- 13 C HMBC, 1 H- 1 H TOCSY, 1 H- 1 H NOESY, and 1 H- 13 C HSQC NMR analysis. Spectra were acquired on a combination of a Bruker Avance III HD 400 MHz spectrometer with a 5 mm BBO 1 H/ 19 F-BB-Z-Gradient prodigy cryoprobe, a Bruker Avance III HD 500 MHz spectrometer with a PA BBO 500S2 BBF-H-D_05 Z SP probe, or a Bruker Avance III HD Ascend 700 MHz spectrometer equipped with a 5 mm triple-resonance Observe (TXO) cryoprobe with Z-gradients. Data were collected and reported as follows: chemical shift, integration multiplicity (s, singlet; d, doublet; t, triplet; and m, multiplet), and coupling constant. Chemical shifts are reported using the DMSO- d_6 : o0 = 2.50 ppm and o13C NMR DMSO-o6: o0 = 39.6 ppm. NMR data were processed using MestReNova v12.0.0–20080.

Hydrolysis and Derivatization of 1 for Labionin Analysis. Lanthipeptide 1 was hydrolyzed and derivatized to confirm the presence of the labionin amino acid moiety following a previously reported method¹⁴ with minor modification. Briefly, 1 mg of 1 was dissolved in 6M HCl (800 μ L) in a 5 mL round-bottom flask. The mixture was refluxed at 110 $^{\circ}\text{C}$ for 24 h before the contents were concentrated to dryness under a gentle stream of N2. The residue was then redissolved in a 2M ethanolic solution (800 μ L) prepared by mixing acetyl chloride with absolute ethanol (1:4, v/v). The solution was refluxed again for 30 min at 110 °C, and the contents were dried again under N2. The residue was then dissolved in dichloromethane (400 μ L), and trifluoroacetic anhydride (200 μ L) was added. The solution was then refluxed for a third time at 110 °C for 10 min before drying under N_2 . Finally, the residue was dissolved in 100 μ L of methanol for HPLC-OrbiTrap analysis. For β -ME derivatization, 1 was incubated with β -ME (6 mM) for 2 h at 30 °C. The reaction mixture was subjected to HPLC-OrbiTrap analysis.

Absolute Configuration Determination of 1. Lanthipeptide 1 (1 mg) was incubated with 6 M HCl (700 μ L) at 115 °C for 10 h for hydrolysis. After concentrating the hydrolysate to dryness under N₂, the residue was resuspended in distilled H_2O (700 μL) and dried again under N₂. This process was repeated three times to completely remove residual acid. The hydrolysate was then divided into two portions for chemical derivatization with 1-fluoro-2,4-dinitrophenyl-5-L-alanine amide (L-FDAA) or 1-fluoro-2,4-dinitrophenyl-5-D-alanine amide (D-FDAA). Each sample was treated with 1 M NaHCO₃ (100 μ L) and either L- or D-FDAA (100 μ L, 1% solution in acetone) at 40 $^{\circ}$ C for 1 h. Then, 1 M HCl (150 μ L) was added to the reaction mixture, and 150 μ L of MeCN was used to dilute the reaction mixture for HPLC-OrbiTrap (Kinetex C18 HPLC column, 4.6 × 100 mm, 2.4 μ m, 100 Å) analysis. A gradient elution from 95 to 38% H₂O/MeCN with constant 0.1% formic acid with a flow rate of 1.0 mL/min over 30 min was applied. Positive and negative ionization modes were used, and UV absorbance was analyzed at 340 nm.

To prepare the FDAA derivatives of amino acid standards, each amino acid (50 mM in $\rm H_2O)$ was made to react with L- or p-FDAA (1% solution in acetone) at 40 °C for 1 h in the presence of 1 M NaHCO_3. The reaction was quenched with 1 M HCl and diluted with MeCN, followed by HPLC-OrbiTrap analysis using the same column and elution condition as described above. L- and p-FDAA derivatives were detected by either UV or extracted ion chromatograms. Absolute configurations of amino acid residues in 1 were established by comparing the retention times of FDAA-derivatized peptide hydrolysate with those of amino acid standards.

Antibacterial Activity Assay. The antibacterial activities of paenithopeptins were measured by the agar diffusion assay. Lanthipeptides 1, 2, 10 and 11 were dissolved in dimethyl sulfoxide (DMSO) and diluted by H₂O to a final concentration of 1 mg/mL. The final concentration of DMSO was 2%. LB agar plates were prepared by diluting overnight-cultured bacterial strains 5000-fold in molten 0.75% LB agar. Then, filter paper discs (diameter 5 mm) were placed on the agar surface, and 2 μ L of paenithopeptin solution was aliquoted onto the filter paper. DMSO in H₂O was used as a negative control, and ampicillin (1 mg/mL) was used as a positive control. Plates were incubated at 30 °C for 24 h. The diameter of the growth inhibition zone was measured and assigned a category ("-", "+", "++", or "+++"), representing the strength of inhibition. "-" indicates no inhibition zone. Growth inhibition zones between 1 and 2 cm correspond to "+". Diameters of inhibition zones between 2 and 3 cm correspond to "++". Growth inhibition zones greater than 4 cm are represented by "+++".

ASSOCIATED CONTENT

Supporting Information

The Supporting Information is available free of charge at https://pubs.acs.org/doi/10.1021/acschembio.2c00849.

Information of primers, plasmids, and strains; LC-MS analysis procedure; 1H , ^{13}C , and 2D NMR as well as HR-ESIMS spectra; in vivo analysis and chemical structure of lanthipeptides (PDF)

Bioinformatic analysis data and methyltransferase information in class III lanthipeptide BGCs listed in the Supplementary data file (XLSX)

■ AUTHOR INFORMATION

Corresponding Author

Jie Li — Department of Chemistry and Biochemistry, University of South Carolina, Columbia, South Carolina 29208, United States; orcid.org/0000-0001-7977-6749; Email: li439@mailbox.sc.edu

Authors

Dan Xue — Department of Chemistry and Biochemistry, University of South Carolina, Columbia, South Carolina 29208, United States; orcid.org/0000-0003-4082-1789

Zhuo Shang — Department of Chemistry and Biochemistry, University of South Carolina, Columbia, South Carolina 29208, United States; Present Address: School of Pharmaceutical Sciences, Shandong University, Jinan, Shandong 250012, China; orcid.org/0000-0002-5755-2629

Ethan A. Older – Department of Chemistry and Biochemistry, University of South Carolina, Columbia, South Carolina 29208, United States

Zheng Zhong — Department of Chemistry and the Swire Institute of Marine Science, The University of Hong Kong, Hong Kong 999077, China; Southern Marine Science and Engineering Guangdong Laboratory (Guangzhou), Guangzhou 519000, China

- Conor Pulliam Department of Chemistry and Biochemistry, University of South Carolina, Columbia, South Carolina 29208, United States
- **Kyle Peter** Department of Chemistry and Biochemistry, University of South Carolina, Columbia, South Carolina 29208, United States
- Mitzi Nagarkatti Department of Pathology, Microbiology and Immunology, School of Medicine, University of South Carolina, Columbia, South Carolina 29209, United States
- Prakash Nagarkatti Department of Pathology, Microbiology and Immunology, School of Medicine, University of South Carolina, Columbia, South Carolina 29209, United States
- Yong-Xin Li Department of Chemistry and the Swire Institute of Marine Science, The University of Hong Kong, Hong Kong 999077, China; Southern Marine Science and Engineering Guangdong Laboratory (Guangzhou), Guangzhou 519000, China; □ orcid.org/0000-0003-4422-2302

Complete contact information is available at: https://pubs.acs.org/10.1021/acschembio.2c00849

Author Contributions

[#]D.X. and Z.S. contributed equally to this work.

Notes

The authors declare no competing financial interest.

ACKNOWLEDGMENTS

This work was partially funded by a National Institutes of Health (NIH) grant P20GM103641 and a National Science Foundation (NSF) EPSCoR Program OIA-1655740. We thank P. J. Pellechia and T. Johnson from the UofSC NMR Facility for help with acquiring NMR data, and we thank M. D. Walla and W. E. Cotham from the UofSC Mass Spectrometry Facility for help with acquiring HRMS and CID-MS/MS data. We thank M. D. Madden (UofSC) for help with data processing.

REFERENCES

- (1) Montalbán-López, M.; Scott, T. A.; Ramesh, S.; Rahman, I. R.; van Heel, A. J.; Viel, J. H.; Bandarian, V.; Dittmann, E.; Genilloud, O.; Goto, Y.; Grande Burgos, M. J.; Hill, C.; Kim, S.; Koehnke, J.; Latham, J. A.; Link, A. J.; Martínez, B.; Nair, S. K.; Nicolet, Y.; Rebuffat, S.; Sahl, H. G.; Sareen, D.; Schmidt, E. W.; Schmitt, L.; Severinov, K.; Süssmuth, R. D.; Truman, A. W.; Wang, H.; Weng, J. K.; van Wezel, G. P.; Zhang, Q.; Zhong, J.; Piel, J.; Mitchell, D. A.; Kuipers, O. P.; van der Donk, W. A. New Developments in RiPP Discovery, Enzymology and Engineering. *Nat. Prod. Rep.* **2021**, 38, 130–239
- (2) Ongpipattanakul, C.; Desormeaux, E. K.; DiCaprio, A.; van der Donk, W. A.; Mitchell, D. A.; Nair, S. K. Mechanism of Action of Ribosomally Synthesized and Post-Translationally Modified Peptides. *Chem. Rev.* **2022**, *122*, 14722–14814.
- (3) Repka, L. M.; Chekan, J. R.; Nair, S. K.; van der Donk, W. A. Mechanistic Understanding of Lanthipeptide Biosynthetic Enzymes. *Chem. Rev.* **2017**, *117*, 5457–5520.
- (4) Hegemann, J. D.; Süssmuth, R. D. Matters of Class: Coming of Age of Class III and IV Lanthipeptides. *RSC Chem. Biol.* **2020**, 1, 110–127.
- (5) Xu, M.; Zhang, F.; Cheng, Z.; Bashiri, G.; Wang, J.; Hong, J.; Wang, Y.; Xu, L.; Chen, X.; Huang, S.; Lin, S.; Deng, Z.; Tao, M. Functional Genome Mining Reveals a Class V Lanthipeptide Containing a d -Amino Acid Introduced by an F420 H2 -Dependent Reductase. *Angew. Chemie* **2020**, *132*, 18185–18191.
- (6) Pei, Z.-F.; Zhu, L.; Sarksian, R.; van der Donk, W. A.; Nair, S. K. Class V Lanthipeptide Cyclase Directs the Biosynthesis of a Stapled Peptide Natural Product. *J. Am. Chem. Soc.* **2022**, *144*, 17549–17557.

- (7) Ortiz-López, F. J.; Carretero-Molina, D.; Sánchez-Hidalgo, M.; Martín, J.; González, I.; Román-Hurtado, F.; Cruz, M.; García-Fernández, S.; Reyes, F.; Deisinger, J. P.; Müller, A.; Schneider, T.; Genilloud, O. C. First Member of the New Lanthidin RiPP Family. *Angew. Chemie Int. Ed.* **2020**, *59*, 12654–12658.
- (8) Müller, W. M.; Schmiederer, T.; Ensle, P.; Süssmuth, R. D. Vitro Biosynthesis of the Prepeptide of Type-III Lantibiotic Labyrinthopeptin A2 Including Formation of a C-C Bond as a Post-Translational Modification. *Angew. Chemie Int. Ed.* **2010**, *49*, 2436–2440.
- (9) Meindl, K.; Schmiederer, T.; Schnieder, K.; Reicke, A.; Butz, D.; Keller, S.; Gühring, H.; Vértesy, L.; Wink, J.; Hoffmann, H.; Brönstrup, M.; Sheldrick, G. M.; Süssmuth, R. D. Labyrinthopeptins: A New Class of Carbacyclic Lantibiotics. *Angew. Chemie Int. Ed.* **2010**, *49*, 1151–1154.
- (10) Xue, D.; Older, E. A.; Zhong, Z.; Shang, Z.; Chen, N.; Dittenhauser, N.; Hou, L.; Cai, P.; Walla, M. D.; Dong, S. H.; Tang, X.; Chen, H.; Nagarkatti, P.; Nagarkatti, M.; Li, Y. X.; Li, J. Correlational Networking Guides the Discovery of Unclustered Lanthipeptide Protease-Encoding Genes. *Nat. Commun.* **2022**, *13*, 1647.
- (11) Walker, M. C.; Eslami, S. M.; Hetrick, K. J.; Ackenhusen, S. E.; Mitchell, D. A.; van der Donk, W. A. Precursor Peptide-Targeted Mining of More than One Hundred Thousand Genomes Expands the Lanthipeptide Natural Product Family. *BMC Genomics* **2020**, *21*, 387.
- (12) Takano, H.; Matsui, Y.; Nomura, J.; Fujimoto, M.; Katsumata, T.; Koyama, I.; Mizuno, S.; Amano, M.; Shiratori-Takano, H.; Komatsu, K.; Ikeda, H.; Ueda, K. High Production of a Class III Lantipeptide AmfS in *Streptomyces Griseus*. *Biosci. Biotechnol. Biochem*. **2017**, *81*, 153–164.
- (13) Völler, G. H.; Krawczyk, J. M.; Pesic, A.; Krawczyk, B.; Nachtigall, J.; Süssmuth, R. D. Characterization of New Class III Lantibiotics-Erythreapeptin, Avermipeptin and Griseopeptin from Saccharopolyspora Erythraea, Streptomyces Avermitilis and Streptomyces Griseus Demonstrates Stepwise N-Terminal Leader Processing. ChemBioChem 2012, 13, 1174–1183.
- (14) Wang, H.; van der Donk, W. A. Biosynthesis of the Class III Lantipeptide Catenulipeptin. ACS Chem. Biol. 2012, 7, 1529–1535.
- (15) Krawczyk, B.; Völler, G. H.; Völler, J.; Ensle, P.; Süssmuth, R. D. Curvopeptin: A New Lanthionine-Containing Class III Lantibiotic and Its Co-Substrate Promiscuous Synthetase. *ChemBioChem* **2012**, 13, 2065–2071.
- (16) Völler, G. H.; Krawczyk, B.; Ensle, P.; Süssmuth, R. D. Involvement and Unusual Substrate Specificity of a Prolyl Oligopeptidase in Class III Lanthipeptide Maturation. *J. Am. Chem. Soc.* 2013, 135, 7426–7429.
- (17) Jungmann, N. A.; van Herwerden, E. F.; Hügelland, M.; Süssmuth, R. D. The Supersized Class III Lanthipeptide Stackepeptin Displays Motif Multiplication in the Core Peptide. *ACS Chem. Biol.* **2016**, *11*, 69–76.
- (18) Chen, S.; Xu, B.; Chen, E.; Wang, J.; Lu, J.; Donadio, S.; Ge, H.; Wang, H. Zn-Dependent Bifunctional Proteases Are Responsible for Leader Peptide Processing of Class III Lanthipeptides. *Proc. Natl. Acad. Sci.* **2019**, *116*, 2533–2538.
- (19) Grigoreva, A.; Andreeva, J.; Bikmetov, D.; Rusanova, A.; Serebryakova, M.; Garcia, A. H.; Slonova, D.; Nair, S. K.; Lippens, G.; Severinov, K.; Dubiley, S. Identification and Characterization of Andalusicin: N-Terminally Dimethylated Class III Lantibiotic from. *Bacillus Thuringiensis Sv. Andalousiensis. iScience* **2021**, 24, 102480.
- (20) Zhang, Y.; Hong, Z.; Zhou, L.; Zhang, Z.; Tang, T.; Guo, E.; Zheng, J.; Wang, C.; Dai, L.; Si, T.; Wang, H. Biosynthesis of Gut-Microbiota-Derived Lantibiotics Reveals a Subgroup of S8 Family Proteases for Class III Leader Removal. *Angew. Chemie Int. Ed.* **2022**, *61*, No. e202114414.
- (21) Shi, Y. M.; Hirschmann, M.; Shi, Y. N.; Ahmed, S.; Abebew, D.; Tobias, N. J.; Grün, P.; Crames, J. J.; Pöschel, L.; Kuttenlochner, W.; Richter, C.; Herrmann, J.; Müller, R.; Thanwisai, A.; Pidot, S. J.; Stinear, T. P.; Groll, M.; Kim, Y.; Bode, H. B. Global Analysis of Biosynthetic Gene Clusters Reveals Conserved and Unique Natural

Products in Entomopathogenic Nematode-Symbiotic Bacteria. *Nat. Chem.* **2022**, *14*, 701–712.

- (22) Covington, B. C.; Xu, F.; Seyedsayamdost, M. R. A Natural Product Chemist's Guide to Unlocking Silent Biosynthetic Gene Clusters. *Annu. Rev. Biochem.* **2021**, *90*, 763–788.
- (23) Rutledge, P. J.; Challis, G. L. Discovery of Microbial Natural Products by Activation of Silent Biosynthetic Gene Clusters. *Nat. Rev. Microbiol.* **2015**, *13*, 509–523.
- (24) Cimermancic, P.; Medema, M. H.; Claesen, J.; Kurita, K.; Wieland Brown, L. C.; Mavrommatis, K.; Pati, A.; Godfrey, P. A.; Koehrsen, M.; Clardy, J.; Birren, B. W.; Takano, E.; Sali, A.; Linington, R. G.; Fischbach, M. A. Insights into Secondary Metabolism from a Global Analysis of Prokaryotic Biosynthetic Gene Clusters. *Cell* **2014**, *158*, 412–421.
- (25) Zhang, X.; Elliot, M. A. Unlocking the Trove of Metabolic Treasures: Activating Silent Biosynthetic Gene Clusters in Bacteria and Fungi. *Curr. Opin. Microbiol.* **2019**, *51*, 9–15.
- (26) Kenshole, E.; Herisse, M.; Michael, M.; Pidot, S. J. Natural Product Discovery through Microbial Genome Mining. *Curr. Opin. Chem. Biol.* **2021**, *60*, 47–54.
- (27) Lee, J.; Hao, Y.; Blair, P. M.; Melby, J. O.; Agarwal, V.; Burkhart, B. J.; Nair, S. K.; Mitchell, D. A. Structural and Functional Insight into an Unexpectedly Selective N-Methyltransferase Involved in Plantazolicin Biosynthesis. *Proc. Natl. Acad. Sci. U.S.A.* **2013**, *110*, 12954–12959.
- (28) Shang, Z.; Winter, J. M.; Kauffman, C. A.; Yang, I.; Fenical, W. Salinipeptins: Integrated Genomic and Chemical Approaches Reveal Unusual d -Amino Acid-Containing Ribosomally Synthesized and Post-Translationally Modified Peptides (RiPPs) from a Great Salt Lake Streptomyces Sp. ACS Chem. Biol. 2019, 14, 415–425.
- (29) Wang, F.; Wei, W.; Zhao, J.; Mo, T.; Wang, X.; Huang, X.; Ma, S.; Wang, S.; Deng, Z.; Ding, W.; Liang, Y.; Zhang, Q. Genome Mining and Biosynthesis Study of a Type B Linaridin Reveals a Highly Versatile α -N-Methyltransferase. CCS Chem **2021**, 3, 1049–1057.
- (30) Abdallah, I. I.; Xue, D.; Pramastya, H.; van Merkerk, R.; Setroikromo, R.; Quax, W. J. A Regulated Synthetic Operon Facilitates Stable Overexpression of Multigene Terpenoid Pathway in Bacillus subtilis. *J. Ind. Microbiol. Biotechnol.* **2020**, 47, 243–249.
- (31) Pesic, A.; Henkel, M.; Süssmuth, R. D. Identification of the Amino Acid Labionin and Its Desulfurised Derivative in the Type-III Lantibiotic LabA2 by Means of GC/MS. *Chem. Commun.* **2011**, *47*, 7401–7403
- (32) Claesen, J.; Bibb, M. Genome Mining and Genetic Analysis of Cypemycin Biosynthesis Reveal an Unusual Class of Posttranslationally Modified Peptides. *Proc. Natl. Acad. Sci. U.S.A.* **2010**, *107*, 16297–16302.
- (33) Saitou, N.; Nei, M. The Neighbor-Joining Method: A New Method for Reconstructing Phylogenetic Trees. *Mol. Biol. Evol.* **1987**, 4, 406–425.
- (34) Tamura, T.; Stecher, S.; Kumar, K. MEGA11: Molecular Evolutionary Genetics Analysis Version 11. *Mol. Biol. Evol.* **2021**, 38, 3022–3027.
- (35) Vellanoweth, R. L.; Rabinowitz, J. C. The influence of ribosome-binding-site elements on translational efficiency in Bacillus subtilis and Escherichia coli in vivo. *Mol. Microbiol.* **1992**, *6*, 1105–1114
- (36) Yeh, C. M.; Chang, H. K.; Hsieh, H. M.; Yoda, K.; Yamasaki, M.; Tsai, Y. C. Improved Translational Efficiency of Subtilisin YaB Gene with Different Initiation Codons in Bacillus Subtilis and Alkalophilic bacillus YaB. J. Appl. Microbiol. 1997, 83, 758–763.
- (37) Bachman, B. Site-Directed Mutagenesis. *Methods Enzym* 2013, 529, 241–248.

☐ Recommended by ACS

Megalochelin, a Tridecapeptide Siderophore from a Talented Streptomycete

Kristiina Vind, Marianna Iorio, et al.

MARCH 15, 2023

ACS CHEMICAL BIOLOGY

READ 🗹

Structural and Biochemical Insights into Post-Translational Arginine-to-Ornithine Peptide Modifications by an Atypical Arginase

Silja Mordhorst, Anna L. Vagstad, et al.

FEBRUARY 15, 2023

ACS CHEMICAL BIOLOGY

READ 🗹

Discovery of Cyclic Lipopeptides Ralstopeptins A and B from *Ralstonia solanacearum* Species Complex and Analysis of Biosynthetic Gene Evolution

Nao Matsukawa, Kenji Kai, et al.

FEBRUARY 22, 2023

ACS CHEMICAL BIOLOGY

READ **C**

Mammalian Commensal *Streptococci* Utilize a Rare Family of Class VI Lanthipeptide Synthetases to Synthesize Miniature Lanthipeptide-type Ribosomal Peptide Natural...

Yile He, Yigang Tong, et al.

DECEMBER 28, 2022

BIOCHEMISTRY

READ 🗹

Get More Suggestions >